Hydrophobic nanopatterning on a flexible gas barrier film by using a poly(dimethylsiloxane) elastomer

Jin-Hwan Choi *et al* 2009 *Nanotechnology* **20** 135303 (5pp) doi: 10.1088/0957-4484/20/13/135303 (Help)

Jin-Hwan Choi, Young-Min Kim, Young-Wook Park, Tae-Hyun Park, Ki-Young Dong and Byeong-Kwon Ju[1]

Display and Nanosystem Laboratory, College of Engineering, Korea University, 5-1, Anam-Dong, Seongbuk-Gu, Seoul 136-713, Korea

[1] Author to whom any correspondence should be addressed

E-mail: bkju@korea.ac.kr

Abstract. In this work, we fabricated a hydrophobic and transparent gas barrier film via a nanopatterned poly(dimethylsiloxane) elastomer imprinting on an ultraviolet-curable polymer resin. A Ca degradation method (water permeation rate) and surface energy measurements were used to determine the level of modification of the surface characteristics. As a result, the decreased surface energy from 25.8 to 7.29 mN m^{-1} led to a lower water vapor transmission rate from 3.06×10^{-1} to 6.24×10^{-2} g m^{-2} day^{-1} according to the degree of decreased Ca height from 100 nm. A tunable wettability is beneficial for application where controlling the direction of moisture flow is important, such as in flexible organic electronics.

Print publication: Issue 13 (1 April 2009)

Received 16 August 2008, in final form 3 February 2009

Published 10 March 2009

Nanotechnology **20** (2009) 135303 (5pp) doi:10.1088/0957-4484/20/13/135303

Hydrophobic nanopatterning on a flexible gas barrier film by using a poly(dimethylsiloxane) elastomer

Jin-Hwan Choi, Young-Min Kim, Young-Wook Park, Tae-Hyun Park, Ki-Young Dong and Byeong-Kwon Ju[1]

Display and Nanosystem Laboratory, College of Engineering, Korea University, 5-1, Anam-Dong, Seongbuk-Gu, Seoul 136-713, Korea

E-mail: bkju@korea.ac.kr

Received 16 August 2008, in final form 3 February 2009
Published 10 March 2009
Online at stacks.iop.org/Nano/20/135303

Abstract

In this work, we fabricated a hydrophobic and transparent gas barrier film via a nanopatterned poly(dimethylsiloxane) elastomer imprinting on an ultraviolet-curable polymer resin. A Ca degradation method (water permeation rate) and surface energy measurements were used to determine the level of modification of the surface characteristics. As a result, the decreased surface energy from 25.8 to 7.29 mN m^{-1} led to a lower water vapor transmission rate from 3.06×10^{-1} to 6.24×10^{-2} g m^{-2} day^{-1} according to the degree of decreased Ca height from 100 nm. A tunable wettability is beneficial for application where controlling the direction of moisture flow is important, such as in flexible organic electronics.

(Some figures in this article are in colour only in the electronic version)

1. Introduction

Water repellence and controlling are important properties of flexible organic devices from both the fundamental and practical aspects [1, 2]. The wetting property of the flat surface is governed by the surface free energy of the material itself. However, some structures such as a lotus leaf in nature show an extremely hydrophobic characteristic [3]. These motivations have led to many research efforts to mimic these biological structures, in particular, the hierarchical structure of a lotus leaf with the contribution of micro/nanotechnologies. Lotus leaves are unusually water repellent and keep themselves spotless. On their surface are countless miniature protrusions coated with a water-repellent hydrophobic substance [3, 4]. Many researchers have focused on fabricating super-hydrophobic surfaces, which are potentially suitable for various applications, such as dust-free and self-cleaning surfaces for solar cells, satellite dishes, complex bioactivities, micro-fluidic channels and prevention of water corrosion [4–9].

The wettability of surfaces is governed by both the surfaces' chemical modifications and geometrical structures. Chemical means such as sol–gel methods [10], fluorination [11] and plasma treatment [12] have been widely used; some of these, however, suffer the drawback of having only a short-lived effect. We suggest, based on our present work, a mass-producible and large-scale fabrication method for hydrophobic and highly transparent gas barrier films by means of a structural modifying process that can maximize productivity and cost effectiveness with a low temperature process.

Water-repellent and barrier properties can be characterized by the moisture permeation measurements. These measurements can be obtained by the Ca degradation method using an electrical detecting system as previously reported [13]. Ca is a highly sensitive material to water vapor. In this measurement, Ca was encapsulated hermetically by the gas barrier film and the water vapor transmission rates (WVTRs) could be derived by measuring the quantity of oxidized Ca after permeation of water vapor passing though the gas barrier film. When Ca, as an electrical conductor, reacts with water vapor, Ca-oxide insulator is formed. So, the electrical resistance of Ca layer is inversely proportional to the amount of decreasing Ca height and we can derive the quantity of oxidized Ca from conductance curve, when constant voltage is applied. We have normalized the initial current value as an initial height

[1] Author to whom any correspondence should be addressed.

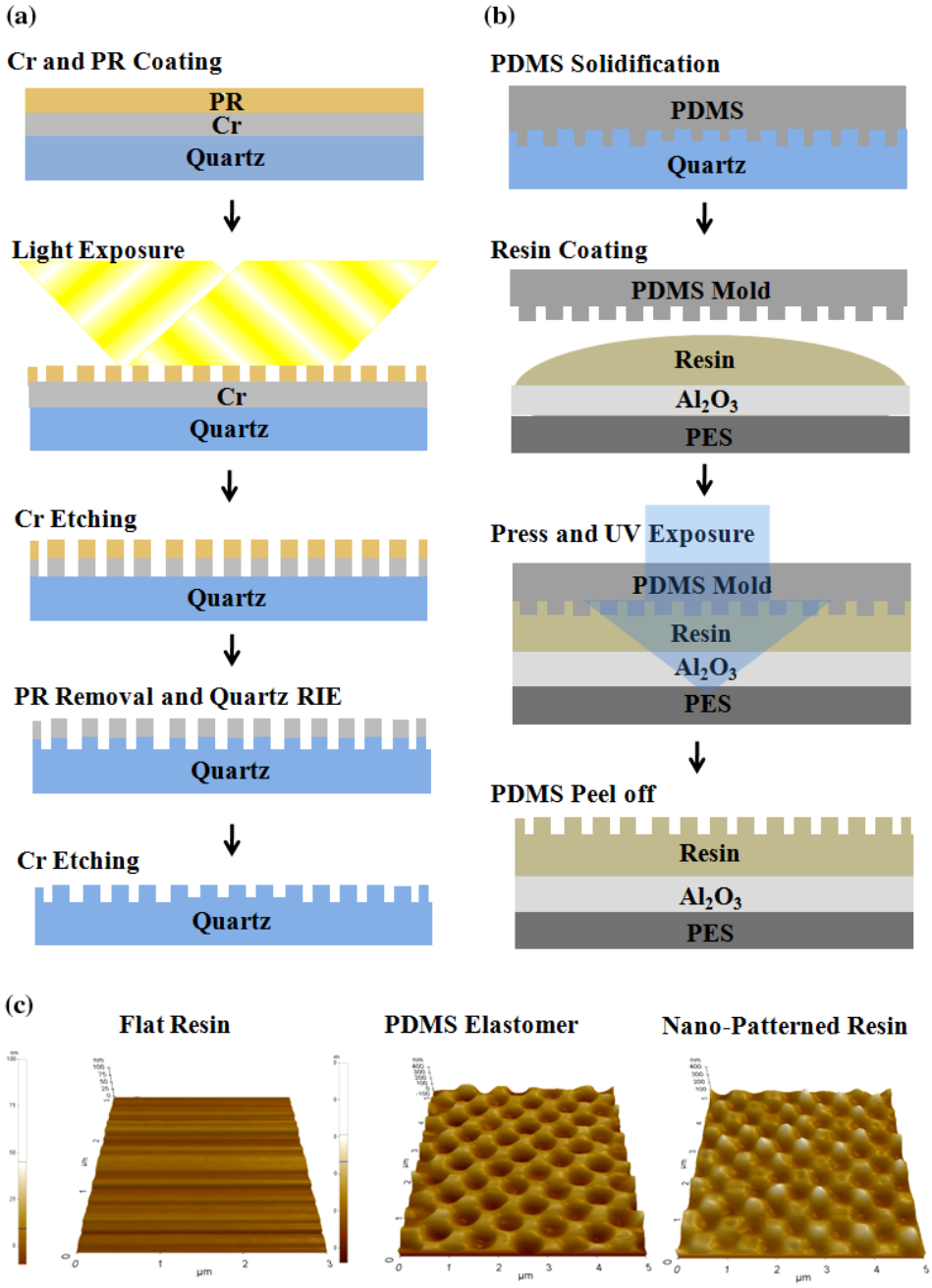

Figure 1. Schematics of (a) the fabrication process of a nanopatterned quartz master, (b) UV-NIL procedure for the direct fabrication of a nanopatterned UV-cured resin surface and (c) AFM images according to each of the surface modifications.

of Ca (100 nm, density: 1.54 g cm^{-3}). Also, the quantity of water vapor passing through the gas barrier could be calculated by using the chemical equation between Ca and H_2O. Ca (molar mass: 40.1 g) needs $2H_2O$ (molar mass: 36 g) to form $Ca(OH)_2$.

2. Experimental details

In the present study, we fabricated a transparent gas barrier film via mimicking the surface structure of the lotus leaf. Also, we introduce a simple fabrication technique based on nano-imprint lithography (NIL) using ultraviolet (UV) rays to cure a polymer with a hydrophobic coating. This method is a highly versatile technique for the fabrication of three-dimensional surface structures [14–16]. NIL techniques, with an elastomer, are useful for the surface texturing of polymer films since polymer structures can be simply fabricated from an elastomer [17]. These techniques are economical and protect the master from contamination during the process. Poly(dimethylsiloxane) (PDMS) elastomer has a fairly low surface energy and provides easy release between the PDMS and the patterned polymer on the substrate.

In this work, we fabricated hydrophobic surfaces by using an inversely patterned PDMS mold and a UV-cured polymer on a flexible gas barrier. At first, the nanopatterned quartz master has been fabricated as schematically shown in figure 1(a). Our

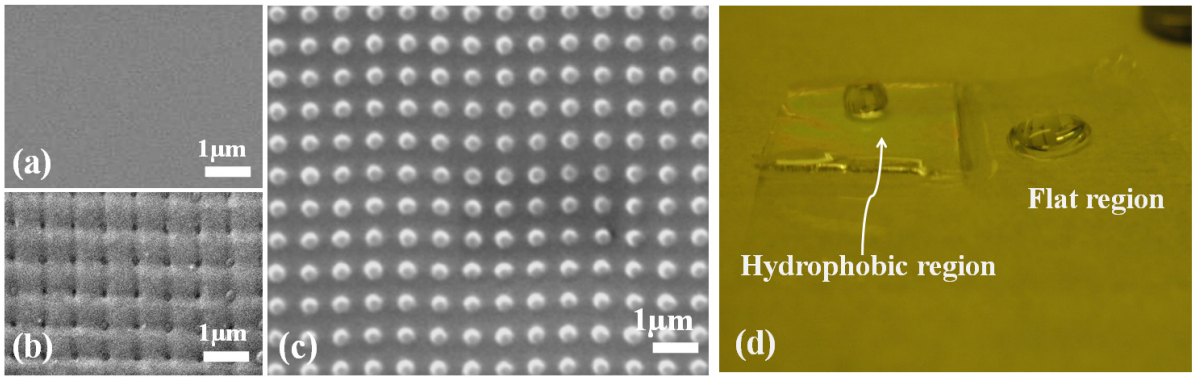

Figure 2. SEM images of (a) a flat UV-cured resin, (b) a negative patterned PDMS elastomer and (c) an imprinted hydrophobic surface. (d) Photo-images of the water droplets on nanopatterned and flat regions.

strategy is to fabricate several master stamps by holographic lithography. The system of laser holography consisted of one laser source (He–Cd, 325 nm wavelength), one beamsplitter, two reflecting mirrors, two beam filters, two collimating lenses and one target. A quartz wafer was used for the stamp preparation. Cr was first deposited over the quartz substrate and a photo-resist (PR) was deposited on top of the Cr layer. Two laser beams separated by a beamsplitter arrived over the resist and printed periodic patterns via an interference phenomenon [18]. The resist was patterned after the laser exposure and was followed by a lift-off process. The chrome layer and the quartz surface were etched by reactive ion etching (RIE) and chrome etchant (CR7SK).

In order to fabricate a PDMS elastomer from a quartz master, we prepared a well-cleaned 4 inch Petri dish and placed the quartz master onto the dish. Then, the PDMS mixture (PDMS:curing agent = 10:1 wt% (Sylgard 184, Dow Corning)) was poured into the dish and kept there for around 30 min in a vacuum desiccator to remove the air bubbles from it and to minimize the air entrapment in the quartz master. Then, the solidification process was carried out in an oven at 70 °C for 6 h. We then carefully used cleaned molds to carry out imprinting on the samples for the wetting property studies.

The thin gas barrier layer was prepared on a polyethersulfone substrate (PES, i-components, 200 μm thickness, 223 °C Tg). It consisted of Al_2O_3 inorganic material and UV-cured resin (Multi-cure 984-LVF, DYMAX Co.). The Al_2O_3 layer was deposited by using an electron beam evaporator below 10^{-6} Torr and then the UV-curable polymer resin was coated by dropping (on a 130 °C hotplate) and spinning (1500 revolutions per minute (RPM), 30 s). The thickness of the UV-cured resin was about 1 μm and the Al_2O_3 inorganic layer was 300 nm. As shown in figure 1(b), an inversely patterned PDMS mold was pressed onto a UV-resin-coated film and the film was exposed to UV light (120 mW cm^{-2} at 365 nm, CURE ZONE HO2, Daeho Glue Tech., Korea). After UV exposure for 2 min followed by baking at 130 °C for 60 min, the PDMS replica mold was peeled off. Finally, this UV-cured resin had the same pattern as the original quartz template.

On the other hand, a flat UV-cured resin layer was first fabricated by flat PDMS imprinting onto UV-resin-coated film and then exposing to UV light. The height of the flat UV-cured resin layer and the average height of the patterned UV-cured resin layer are the same. There was no leakage flow of resin during the imprinting process. The surface morphologies of the case in point of these films were analyzed by atomic force microscopy (AFM) as shown in figure 1(c).

According to Owen's equation [19], the surface energy can be calculated from the contact angle measurement of water and formamide. Owen's equation can be expressed as

$$1 + \cos\theta = 2\sqrt{\gamma_s^d}\left(\frac{\sqrt{\gamma_l^d}}{\gamma_l^d + \gamma_l^h}\right) + 2\sqrt{\gamma_s^h}\left(\frac{\sqrt{\gamma_l^h}}{\gamma_l^d + \gamma_l^h}\right) \quad (1)$$

where γ_s^d and γ_l^d are dispersion forces of the solid and the liquid free energy. γ_s^h and γ_l^h indicate the hydrogen bonding of the solid and the liquid free energy. The total energy at a surface is the sum of the contribution from the different intermolecular forces at the surface. γ_l^d and γ_l^h of water and formamide can be attained from previous reports [19–21]. Thus, the surface energy of a solid expressed by

$$\gamma_s = \gamma_s^d + \gamma_s^h \quad (2)$$

can be calculated from the contact angles of water and formamide.

3. Results and discussion

The dimensional quality of the fabricated PDMS negative mold and UV-polymer resin replica were characterized by a scanning electron micrograph (SEM). Figure 2 shows SEM images of (a) a flat UV-cured resin surface, (b) an inversely patterned PDMS mold and (c) a nanopatterned UV-cured resin replica from the imprint method. Dot-like structures existing on the protruding nanopatterns were about 400 nm in width and about 200 nm in depth. Figure 2(d) shows photo-images of the water droplets on nanopatterned and flat surfaces.

In previous works, super-hydrophobic characteristics could be demonstrated by the sub-micrometer-sized texturing process which is smaller and almost the same scale as that of the original lotus leaf. Smaller pattern size and higher aspect ratio can lead to lower surface energy. In this work,

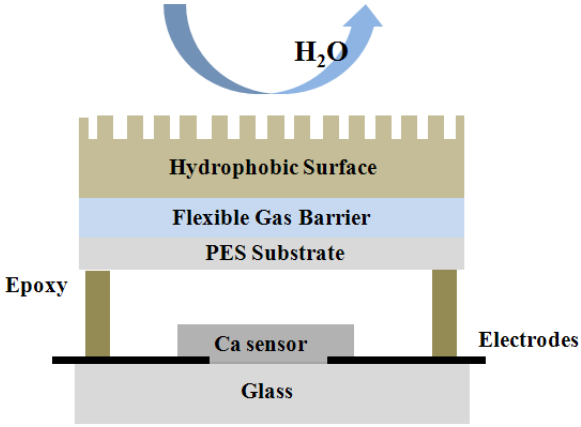

Figure 3. A schematic diagram of the Ca degradation test.

the vapor barrier characteristics have been dependent on the pattern uniformity, freedom from distortion, pinholes and cracks, rather than scale of the pattern subject to the range below 1 μm. As one of the barrier materials, UV-cured resin for use in this work showed better pattern uniformity in the size range of −400 and 700–800 nm center to center, the same as in this work. Also, it showed a better pattern transfer property from the PDMS mold to the surface of UV-cured resin.

The schematic diagram of the Ca test for measurements of WVTRs is shown in figure 3. We calculated the WVTRs as below:

$$\mathrm{WVTR} = 33.181 \times 10^6 \times \left(1 - \frac{R_\mathrm{i}}{R}\right)\frac{h_\mathrm{i}}{\mathrm{hrs}} \qquad (3)$$

where h denotes the Ca height, R is the resistance of the thin Ca layer connected to the electrodes and R_i are h_i initial values of R and h. The WVTR is proportional to the conductance which is indicated by a decrease in the Ca height Δh versus the elapsed time 'h'. Previously, the WVTRs for the bare PES (34.1 g m^{-2} day^{-1}) and Al_2O_3-coated PES (0.86 g m^2 day^{-}1 with the root mean square (RMS) roughness of 1.526 nm) was measured at 20 °C and 60% relative humidity (RH).

In figure 4(a), we can see changes in the electrical transmission through the thin Ca. At 20 °C and 60% RH, the permeation curve of PES coated with flat UV-cured resin indicated that the Ca layer at a height of 100 nm was totally oxidized by water vapor for ∼12 h. We measured a permeation rate with a value of 3.06 × 10^{-1} g m^{-2} day^{-1} consistent with the WVTR derivation. To demonstrate the behavior of a hydrophobic water-repellent characteristic, the permeation rate of the nanopatterned UV-cured resin on the gas barrier film was measured with the same conditions. As a result, the nanopatterned surface showed a better barrier performance with a permeability value of 6.24 × 10^{-2} g m^{-2} day^{-1}. The measurements of Ca degradation by using electrical properties and the permeation rates were calculated by a change of the entire resistance of Ca. Therefore, the slope of current versus elapsed time was linear and represented the average permeation rate.

In addition, surface wettability is generally characterized by measuring the contact angle (CA) of a liquid droplet

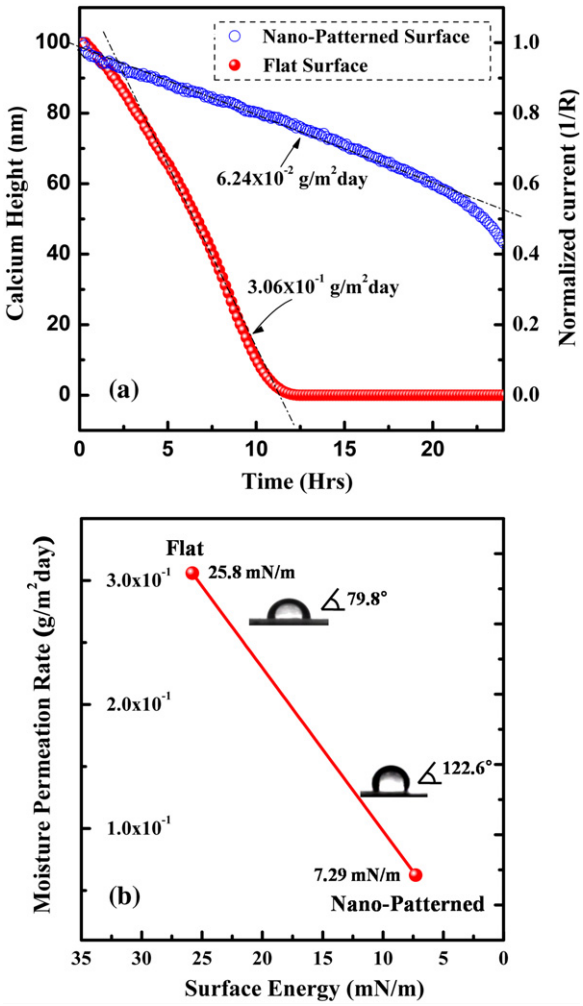

Figure 4. (a) Permeation rates measurement for PES films coated with flat and hydrophobic nanopatterned UV-cured resin on 300 nm Al_2O_3 barrier layers. The slope of the linear fit (dashed line) of the films yields the WVTRs, 3.06 × 10^{-1} g m^{-2} day^{-1} and 6.24 × 10^{-2} g m^{-2} day^{-1} at 20°C and 60% RH, respectively. (b) A change of permeation rate due to surface energy. The DI water CA was changed from 122.6° to 79.8° leading to a decrease in the permeation rate.

sitting on the surface. A static CA measurements system (Phoenix 450, Surface Electro Optic Co. Ltd, Korea) was used to measure the surface wetting properties of the imprinted polymer films. A deionized (DI) water droplet (20 μl) was gently deposited on the sample surface using a micro-pipette. A photograph of the water droplet was taken immediately with a CCD camera. Figure 4(b) shows comparisons of the water CA of the films. The CA of the nanopatterned gas barrier films was 122.6° ± 1.5° compared to a flat surface whose value was 79.8° ± 1.3°. CA values were given by the software. The decrease in surface energy is caused by the change of the surface roughness. The CA was high and close to the original lotus leaf characteristic, resulting in a hydrophobic surface. About formamide, the CA of 72.8° ± 1.1° is on the flat surface and 110.2° ± 1.4° is on the nanopatterned surface. In this case, the increase in the CA was mainly due to the reduction of the surface energy from 25.8 to 7.29 mN m^{-1} according

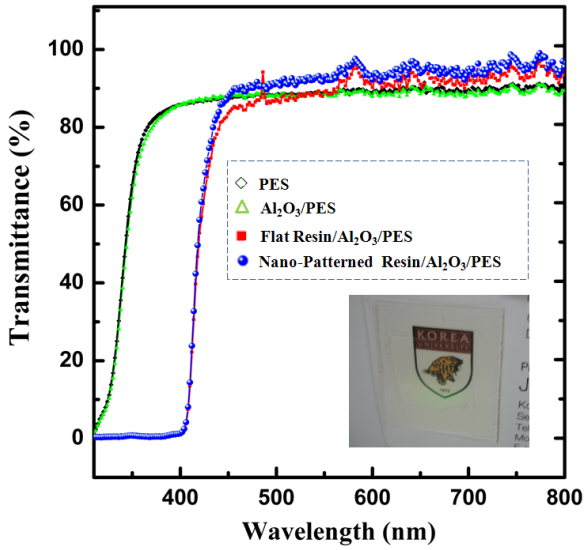

Figure 5. The transmittance of the highly transparent hydrophobic gas barrier and a photo-image of the card underneath the film.

to Owen's equation. The change of surface roughness led to the change of surface energy and enhancement of moisture-repellent characteristics.

Figure 5 represents the transmittance spectrum in the visible region for the replicated film after PDMS molding with references to the bare PES, the Al_2O_3 monolayer and the flat UV-cured resin layer. The transmittance of the hydrophobic film (UV-cured resin replica) on the PES and the references were measured by a UV–vis spectrometer. The Al_2O_3 monolayer on the PES almost had the same transmittance value as the bare PES, above 85% in a wavelength range of approximately from 400 to 800 nm. This graph shows that the UV-cured resin absorbed the UV light in a range of about 220–420 nm. The transmittance of the nanopatterned gas barrier film was higher than that of the bare PES substrate in a region of above 450 nm. After due consideration of Mie scattering theory [22] and highly transparent properties attributed to nanoscale patterning fabrication, this film showed a transmittance value on average of ∼92% for the wavelength range from 450 to 800 nm. These nanopatterned surfaces, with hydrophobic gas barrier properties, are useful for various optical applications. The inset image of figure 5 shows the clearly transparent image of the film on the RGB card.

4. Conclusion

Here, we describe a technique for the direct nanopatterning of a flexible gas barrier substrate. The advantages of this method are its capabilities for generating device patterns on a nanometer scale, using a simple, rapid and non-destructive process with durability. This concept can be effective for the design of gas barrier films with enhanced performance. Therefore, as for the mass production of a hydrophobic gas barrier using polymeric materials, we recommend using an intrinsically organic/inorganic stack that can have more enhancing gas barrier characteristics. We also mention that this promising technique could be widely used in the field of bio-mimicking using surface replication and conventional electroforming technology. In summary, in our work, we demonstrated a highly transparent hydrophobic surface fabrication strategy using NIL with a flexible mold. Our approaches are very suitable for various applications that require both hydrophobic and highly transparent coatings.

Acknowledgments

This work was supported by a Grant-in-Aid (10030041-2008-12) for Next-Generation New Technology Development Programs from the Ministry of Knowledge Economy of Korean Government, and supported by the National Research Laboratory (R0A-2007-000-20111-0) Program of the Ministry of Education, Science and Technology (Korea Science and Engineering Foundation), and this work was supported by the Korea Science and Engineering Foundation (KOSEF) grant funded by the Korea Ministry of Education, Science and Technology (MEST) (No. R11-2007-045-01003-0). JHC thanks the Seoul Metropolitan Government for the Seoul Fellowship.

References

[1] Weaver M S *et al* 2002 *Appl. Phys. Lett.* **81** 2929–31
[2] Chwang A B *et al* 2003 *Appl. Phys. Lett.* **83** 413–5
[3] Blossey R 2003 *Nat. Mater.* **2** 301–6
[4] Lee S and Kwon T H 2007 *J. Micromech. Microeng.* **17** 687–92
[5] Zhai L, Berg M C, Cebeci F C, Kim Y, Milwid J M, Rubner M F and Cohen R E 2006 *Nano Lett.* **6** 1213–7
[6] Han J T, Kim S and Karim A 2007 *Langmuir* **23** 2608–14
[7] Lam P, Wynne K J and Wnek G E 2002 *Langmuir* **18** 948–51
[8] Jeyaprakash J D, Samuel S, Ruther P, Frerichs H P, Lehmann M, Paul O and Ruhe J 2005 *Sensors Actuators* B **110** 218–24
[9] Liu T, Yin Y, Chen S, Chang X and Cheng S 2007 *Electrochim. Acta* **52** 3709–13
[10] Shi M, Xi J, Wang H and Wu X 2008 *J. Adhes. Sci. Technol.* **22** 311–8
[11] Colorado R and Lee T R 2003 *Langmuir* **19** 3288–96
[12] Kim C S, Jo S J, Kim J B, Ryu S Y, Noh J H, Baik H K, Lee S J and Kim Y S 2007 *Appl. Phys. Lett.* **91** 063503
[13] Choi J H, Kim Y M, Park Y W, Huh J W, Kim I S, Hwang H N and Ju B K 2007 *Rev. Sci. Instrum.* **78** 064701
[14] Zhang F and Low H Y 2007 *Langmuir* **23** 7793–8
[15] Kim Y S, Suh K Y and Lee H H 2001 *Appl. Phys. Lett.* **79** 2285–7
[16] Kim C, Burrows P E and Forrest S R 2000 *Science* **288** 831–3
[17] Kim M, Kim K, Lee N Y, Shin K and Kim Y S 2007 *Chem. Commun.* **2237** 9
[18] Murillo R, van Wolferen H A, Abelmann L and Lodder J C 2005 *Microelectron. Eng.* **78** 260–5
[19] Owens D K and Wendt R C 1969 *J. Appl. Polym. Sci.* **13** 1741–7
[20] Fowkers F M 1964 *Indust. Eng. Chem.* **56** 40–52
[21] Kim J S, Friend R H and Cacialli F 1999 *J. Appl. Phys.* **86** 2774–8
[22] Mie G 1908 *Ann. Phys.* **25** 377–91